MSc in Photonics

PHOTONICS**BCN**

Universitat Politècnica de Catalunya (UPC)
Universitat Autònoma de Barcelona (UAB)
Universitat de Barcelona (UB)
Institut de Ciències Fotòniques (ICFO)

http://www.photonicsbcn.eu

Master in Photonics

MASTER THESIS WORK

EFFECT OF ELECTRON-PHONON COUPLING ON THE LIFETIMES OF PLASMONS IN GRAPHENE NANOISLANDS

José Ramón Martínez Saavedra

Supervised by Dr. F. Javier García de Abajo, (ICFO)

Presented on 9th September 2014

Registered at

Escola Tècnica Superior d'Enginyeria de Telecomunicació de Barcelona

Effect of electron-phonon coupling on the lifetimes of plasmons in graphene nanoislands

José Ramón Martínez Saavedra

ICFO-The Institute of Photonic Sciences, Av. Carl Friedrich Gauss, 3, 08860 Castelldefels, Barcelona - SPAIN

E-mail: jrmsaavedra@gmail.com

Abstract. We show that the electron-phonon coupling in graphene planar nanostructures gives rise to an enrichment of the absorption spectra around the plasmonic resonances that these structures can support. Furthermore, we estimate the influence of coupling to phonons over the lifetime of these plasmons. In this line, we compute some values of the inelastic damping rate due to this electron-phonon coupling for graphene nanoislands. We conclude that the electron-phonon coupling channel is in general weaker that impurity scattering, and that gives rise to plasmon broadening in the meV range for large structures, whereas for small ones it has a fundamental role in the lifetime of molecular plasmons.

1. Introduction

Plasmonics has emerged in nowadays photonics as a very promising field, thanks to the attractive properties of plasmons (the collective oscillations of free electrons inside a material) when they interact with light. Features such as sub-wavelength confinement [1] and structural tunability [2] give rise to many applications of plasmons in nanophotonics, such as nano-sensing of small structures [3], nano-focusing of the light fields far beyond the diffraction limit [4], and even the engineering of nanoantennas in the IR, visible and UV regimes [5].

Typical plasmonic materials, such as gold, silver and aluminum, have been the breeding ground for plasmonic science: most research on the early stages of the field has been done with these materials [6], and even nowadays they are a very active field within plasmonics [7]. Withal, these materials have some shortfalls which limit their possible scope of applications, such as high losses and the difficulty of tuning the resonance frequency once the geometry of the structure is fixed.

Because of that, current research is focused on new materials that overcome these limitations. Among them, graphene has arisen as an outstanding alternative to noble metals, thanks precisely to its high tunability capabilities [8] and to the low plasmonic losses when compared with typical plasmonic materials [9]. Even if graphene plasmonic resonances are not in the visible range, but in the terahertz regime, it is a very active and

growing discipline inside plasmonics, with plenty of publications from both theoretical and experimental groups [10].

Because of this intense research activity in the field a host of theoretical issues are matters of debate, such as the origin of plasmon losses in graphene: a topic for which, to our knowledge, there is still no definitive answer so far, despite some works in the literature [11]. However, there is some consensus about the possible plasmon decay channels in graphene, and typically four possibilities are considered: decaying to edge states, electron-hole pair generation, scattering with lattice impurities and coupling to phonon modes [12].

Edge states effects are only important in case of small graphene nanostructures, whose edge's terminations dramatically change the influence of this channel over the total decay rate [13]. Electron-hole pair generation is the dominant decay channel when it is open: nevertheless, due to energy-momentum conservation, this channel is only available for high frequencies, and therefore it is not the dominant one for the IR regime in which we focus on. The lattice impurities are typically derived from calculations of the DC graphene conductivity, using the Drude model [11] or other expressions for the conductivity [14]. The last one, the possibility of coupling to the vibration modes of the atoms by electron-phonon interaction and its contribution to the plasmon lifetime, although discused in some works [11], is still an open question.

The aim of this work is shedding some light over the effects of phonons over the optical response of graphene nanostructures: we use a bottom-up approach, based on the plasmonic properties of polycyclic aromatic hydrocarbons (PAHs)[15]. These molecules (which can be treated as very small graphene nanostructures) also support plasmon resonances in near infrared, visible and UV range. These resonances share some interesting properties with graphene plasmons, such as their high tunability. Moreover, the resonances of these PAHs depend strongly on their size and shape, and they converge to those that appear in infinite graphene for very large structures, so any trend about the electron-phonon coupling behavior when increasing the ensemble size may be extended straightforward to larger graphene structures.

This master thesis starts with an outline of the required theory to go from the hamiltonian for a PAH to an expression for the inelastic damping rate due to phonon generation. Once the basic equations are introduced, the calculation scheme is shown together with some results of the expected plasmon losses due to phonons for small structures. We also study the dependence of the phonon decay channel width with the number of atoms and the shape, and infer the behavior of the losses when dealing with larger graphene nanostructures.

2. Outline of the theory

2.1. Modelling the PAH molecule and its vibrations

In this work we model the molecules as a set of N carbon atoms placed at positions $\mathbf{R}_i$. Their electronic structure is simplified by only considering a $2p_z$ orbital per atom and neglecting the effect of the bounding σ orbitals, which are too deep in the energy diagram to play a significant role when dealing with the optical properties of the molecule [16].

After customary approximations within molecular physics, such as the Born-Oppenheimer approximation [17], we can treat (up to first order) the electronic response of the molecule and the vibrations of the atomic ensemble separatedly: the former is described by means of a tight-binding formalism [18], whereas the latter is treated within the harmonic approximation to lattice vibrations: the total hamiltonian of the system is written within a second quantization formalism as

$$\hat{H} = \hat{H}_{\mathrm{TB}} + \hat{H}_{\mathrm{ph}} = \sum_{l,l'} t_{ll'} \hat{c}_l^\dagger \hat{c}_{l'} + \sum_n \hbar\omega_n \hat{b}_n^\dagger \hat{b}_n \tag{1}$$

where the first sumatory (the tight-binding hamiltonian for the $2p_z$ orbitals) is written in the localized electrons basis (i.e. $\hat{c}_l$ destroys an electron in atom l, and $\hat{c}_l^\dagger$ creates it), and the second one is written in terms of the vibrational eigenstates of the system, with $\hat{b}_n^\dagger, \hat{b}_n$ exciting/destroying a quantum of vibration with energy $\hbar\omega_n$. The parameters $t_{ll'}$ are called *hopping constants*, and they are written in terms of the electronic wave functions φ_{2p_z} and the electrostatic interaction hamiltonian of all the ensemble $\Delta U(\mathbf{r})$ as

$$t_{ll'} = \int_\Omega \mathrm{d}\mathbf{r}\ \varphi^*_{2p_z}(\mathbf{r} + \mathbf{R}_l) \Delta U(\mathbf{r}) \varphi_{2p_z}(\mathbf{r} + \mathbf{R}_{l'}) \tag{2}$$

where the atomic positions $\mathbf{R}_l$ are considered, up to this order, to be fixed at the equilibrium points $\mathbf{R}_l \approx \mathbf{R}_{l,0}$. The coupling with the lattice vibrations arises if we consider these atomic positions not to be fixed, but to have a first-order contribution from the vibrational state of the system: therefore, the hopping is expanded as well up to first order in the atomic positions as

$$\hat{H}_{\mathrm{TB}} = \sum_{l,l'} t_{ll'} \hat{c}_l^\dagger \hat{c}_{l'} \approx \sum_{l,l'} t^0_{ll'} \hat{c}_l^\dagger \hat{c}_{l'} + \sum_{l,l',n} d_{ll'n} \hat{c}_l^\dagger \hat{c}_{l'} \left(\hat{b}_n^\dagger + \hat{b}_n \right) = \hat{H}^0_{\mathrm{TB}} + \hat{H}_{\mathrm{e-ph}} \tag{3}$$

If an external electric field is now applied to the system, as it is the case with external illumination, an additional interaction term is added to the hamiltonian: in the localized orbitals basis, it is a diagonal term and it reads

$$V^{\mathrm{light}} = -e \sum_l (\phi_l^{\mathrm{ext}} + \phi_l^{\mathrm{ind}}) \hat{c}_l^\dagger \hat{c}_l \tag{4}$$

where the induced charge density effects due to the presence of the disturbing external electric field has been included inside the hamiltonian, making it a self-consitent interaction with the electrostatic field.

Therefore, the total system's hamiltonian is finally written, in the states basis of H_0, as

$$H = \underbrace{\sum_{j=1}^{N} \hbar\varepsilon_j \hat{a}_j^\dagger \hat{a}_j + \sum_{n=1}^{N} \hbar\omega_n \hat{b}_n^\dagger \hat{b}_n}_{H^0} + \underbrace{\sum_{j,j'} \hat{a}_j^\dagger \hat{a}_{j'} \left(-e\phi_{jj'} + W_{jj'n}\left(\hat{b}_n + \hat{b}_n^\dagger\right)\right)}_{H^{\text{int}}} \tag{5}$$

where now $\hat{a}_j^\dagger$ creates an electron in the collective state j, $\hat{a}_j$ destroys it, and $W_{jj'n}$, $\phi_{jj'}$ are the coefficients of the electron-phonon coupling and the external electrostatic interaction in this new basis.

2.2. Inelastic damping rate of plasmons due to electron-phonon coupling

Once an expression for the perturbative hamiltonian is found, estimating the wave function by means of perturbation theory is straightforward, even if we deal with two perturbations instead of one. To take that into account, the wave function is expanded in terms of both perturbations as

$$|\psi\rangle = |\psi_{00}\rangle - e\,|\psi_{10}\rangle + \alpha\,|\psi_{01}\rangle - e\alpha\,|\psi_{11}\rangle + \cdots \tag{6}$$

where $(-e)^i\alpha^j\,|\psi_{ij}\rangle$ is the perturbative expansion of the wave function that corresponds to i perturbations in the self-consistent electrostatic potential $\hat{\phi}^{\text{tot}}$ and j in the electron-phonon coupling term $\hat{W}$ As the simplest description of our molecular system, we assume that the ground state of the unperturbed electronic system is that of a Fermi liquid, with all electronic levels filled up to a certain chemical potential μ. In the case of the vibrational levels, the high energies of the optical phonons when compared with the thermal average energy k_BT alllows us to assume that there are no phonons in the ground state of the system. With these assumptions, we build the unperturbed ground state of the whole system as

$$|G\rangle = |g\rangle \otimes |\mathbf{0}\rangle \tag{7}$$

From here, we can start a perturbative expansion of the wave function: setting the ground state as the energy origin ($H_0\,|G\rangle = 0\,|G\rangle$), we find expressions for the different wave functions by means of standard time-dependent perturbation theory. Assuming a monochromatic, adiabatically switched electrostatic potential $\phi_{jj'}(t) = 2\phi_{jj'}e^{\delta t}\cos(\omega t)$, and using the Rotating Wave Approximation whenever possible, we find

$$|\psi_{00}\rangle = |G\rangle \qquad |\psi_{10}\rangle = \sum_{j>j'} \frac{\phi_{jj'}}{\hbar\left(\omega - (\varepsilon_j - \varepsilon_{j'}) + \mathrm{i}\delta\right)} e^{-\mathrm{i}(\omega+\mathrm{i}\delta)t} \hat{a}_j^\dagger \hat{a}_{j'}\,|G\rangle \tag{8}$$

For the calculation of the $|\psi_{01}\rangle$ correction, we first focus on the perturbed state of the system: since the electronic state is that of a Fermi sea ground state and, therefore, all levels beyond the chemical potential are occupied, there is no possibility that a phonon can be emitted from the system due to Pauli's exclusion principle. On the other

hand, since there are no phonons in the system, no absorption mechanism can happen: therefore, this correction to the wave function has to be zero.

Finally, collecting all the previous results and taking into account that no phonons can be absorbed by the electronic system, we can derive an expression for the $|\psi_{11}\rangle$ term as

$$|\psi_{11}\rangle = -\frac{e^{-\mathrm{i}\chi(t)}}{\hbar^2}\sum_n\left[\frac{B_n}{\omega_n-\omega-\mathrm{i}\delta}+\sum_{j>j'}\frac{C_{jj'n}}{\varepsilon_j-\varepsilon_{j'}+\omega_n-\omega-\mathrm{i}\delta}\hat{a}_j^\dagger\hat{a}_{j'}\right]\hat{b}_n^\dagger|g\rangle \tag{9}$$

where the different coefficients B_n and $C_{jj'n}$ can be written in terms of the e-ph coupling constants and the external potential parameters as

$$B_n = \sum_{j\neq j'}(1-f_j)f_{j'}A_{jj'}W_{j'jn} \tag{10}$$

$$C_{jj'n} = (1-f_j)f_{j'}\sum_{j''\neq j,j'}\left[(1-f_{j''})A_{j''j'}W_{jj''n}-f_{j''}A_{jj''}W_{j''j'n}\right] \tag{11}$$

Once the wave function is found, the calculation of the inelastic damping rate due to the presence of phonons is directly calculated by means of Fermi's golden rule [19], which for $\delta\to 0$ reads

$$\gamma = \frac{2\pi e^2}{\hbar^4}\sum_n\left[|B_n|^2\,\delta(\omega_n-\omega)+\sum_{j>j'}|C_{jj'n}|^2\,\delta(\varepsilon_j-\varepsilon_{j'}+\omega_n-\omega)\right] \tag{12}$$

where each term above is associated with a different physical process:

- The former represents the absorption of a photon directly by a vibration: this process, although mediated by the electrons, leaves the electronic state unchanged.
- The latter represents the absorption of the photon by an electron: the final state is that in which a vibration mode is excited and the electron changes its electronic states

A picture of these processes in terms of configuration diagrams is shown in figure 1.

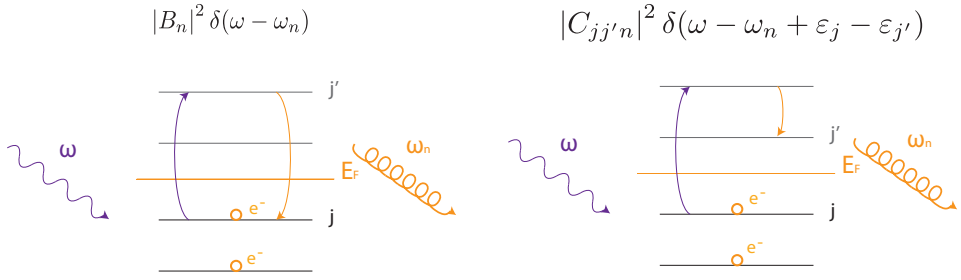

Figure 1. Physical diagramatic explanation of the terms that appear in (12). In both cases, a photon of frequency ω is absorbed and a phonon of frequency ω_n is created.

3. Results and discussion

The calculation of the phonon damping rate from (12) cannot be done numerically due the zero-width of the Dirac delta. In order to avoid that, the delta function is substituted by a lorentzian with a FWHM δ. In order to make the whole procedure self-consistent, we assume that δ is equal to the lifetime of the plasmon $\Gamma = \gamma + \Gamma^{\mathrm{r}}$, where γ is the inelastic damping rate due to phonons and Γ^{r} is the damping rate associated with all the other possible decay channels. The self-consistent equation to be solved is

$$\Gamma = \gamma(\Gamma) + \Gamma^{\mathrm{r}} \longrightarrow f(\Gamma) \equiv \frac{\gamma(\Gamma)}{\Gamma} = 1 - \frac{\Gamma^{\mathrm{r}}}{\Gamma} \tag{13}$$

so once $f(\Gamma)$ is calculated for the resonances we are interested we can obtain the total damping rate of the system Γ and the phonons contribution γ as a function of the rest of contributions to the total damping rate Γ^{r}.

3.1. Results for nanotriangles

In the case of nanotriangles, the electronic structure of the sample shifts smoothly when increasing the size of the nanostructure: therefore, when we analyze the absorption cross-section we see that the resonances shift to lower frequencies when the size of the triangle is increased, as it is shown in figure 2. In this case, only the resonance with the bigger cross-section is studied by means of the formalism derived in section 2.

Applying a self-consistent procedure to (13) we can find results for the total damping rate Γ as a function of just the phonons contribution γ for different γ/Γ ratios: these results are plotted in figure 3(a) as a function of the number of atoms in the structure. Trivially, knowing the value of Γ as well as the γ/Γ ratio we can obtain γ as a function of the ratio and the number of atoms, as shown in figure 3(b). From both figures, it is clear that there is a marked trend of the damping rate to decrease when increasing the size of the triangle: also, the phonon damping decreases when increasing the number of atoms.

Analyzing the results from figure 3(a), it seems to be an upper limit to the maximum influence of the electron-phonon interaction over the total damping rate: for bigger ratios, the self-consistent procedure does not converge.

For completeness, and as an additional way to compare these structures, the Q-factor of the resonances is calculated. This parameter, defined as $Q = \omega\tau = \omega/\Gamma$, gives a measure of the similarity of the resonance with a perfect monochromatic harmonic oscillator: the higher the Q-factor, the better the analogy. However, as it can be seen in figure 3(c), the overall quality of the resonances is not so good, and even falls when increasing the number of atoms, meaning that the narrowing of the resonance when increasing the triangle's size is not fast enough to compensate its redshift.

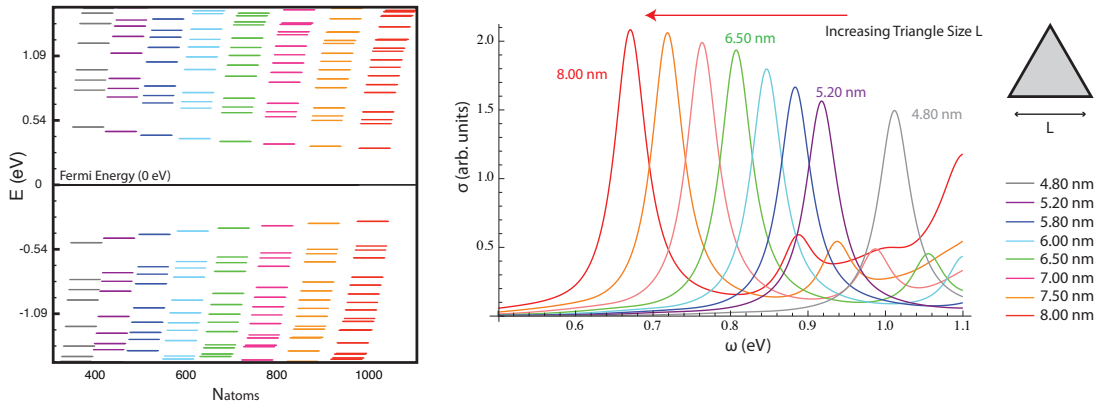

Figure 2. States diagrams (left) and absorption cross-sections (right) for nanometer-sized carbon triangles. The smooth variations in the state distribution result in an smooth displacement of the resonances in the IR regime.

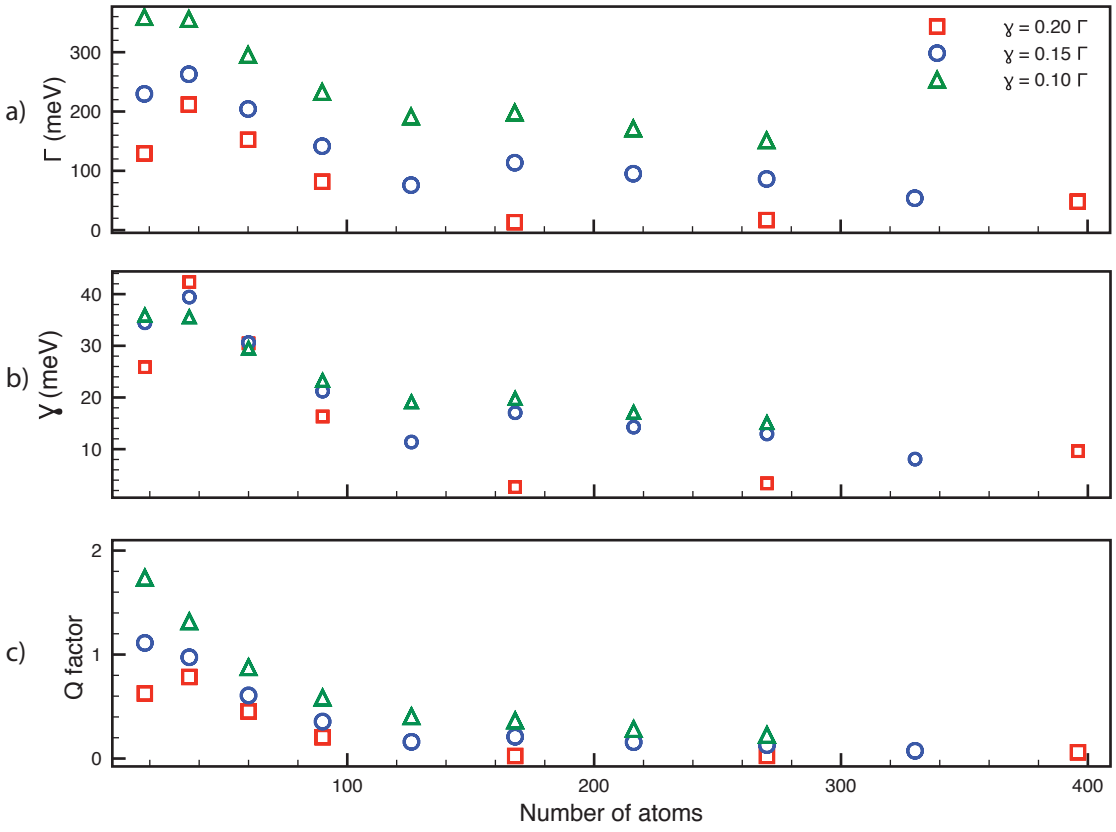

Figure 3. Calculations for the total inelastic damping rate 3(a), the phonon inelastic damping rate 3(b) and the Q-factor 3(c) of the resonances under study.

3.2. Results for nanodisks

In the case of nanodisks, when looking at the electronic structure we can see that it is strongly dependent on the number of atoms, because of edge effects that not all the rounded structure have. However, there is still the possibility to distinguish between three different families of nanodisks, with comparable electronic structure: these families, arbitrarily named *red*, *green* and *blue*, have similar absorption cross-sections when they are calculated, as shown in figure 4. These structural differences have been taken into account when calculating the phonon damping effects, as figures 5(a) and 5(b) show. They also show, as in the nanotriangles case, that the damping effects decrease when increasing the diameter of the disks for all three families, although there are still some differences between them.

Nonetheless, there is a huge difference when compared with the nanotriangles case: for disks, the self-consistency method almost always finds a solution, even if we consider that the whole origin of the damping is just the phonons contribution ($\gamma = \Gamma$): therefore, it seems that the applicability of the self-consistency procedure may be restricted depending on the electronic structure of the system.

Also, for the same reasons as before, we present the Q-factors of the resonances for disks within figure 5(c). In this case the Q-factors are much higher: furthermore, they seem to increase as well with the number of atoms for some of the resonances.

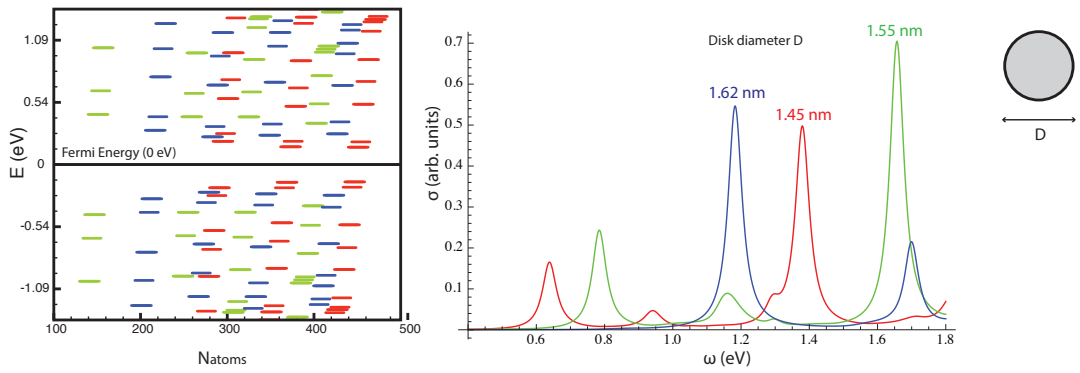

Figure 4. States diagrams (left) and absorption cross-sections of three different nanometer-sized carbon disks (right). Small variations in the diameter produce huge differences among cross-sections, resulting in the appearance of three different families of disks.

4. Conclusions

Throughout this master thesis we have developed a simple, yet consistent method for calculating the contributions of the electron-phonon coupling inside planar carbon nanostructures to the lifetime of the plasmons that these structures support. Due to space limitations, an in-depth description and derivation of the theory couldn't be

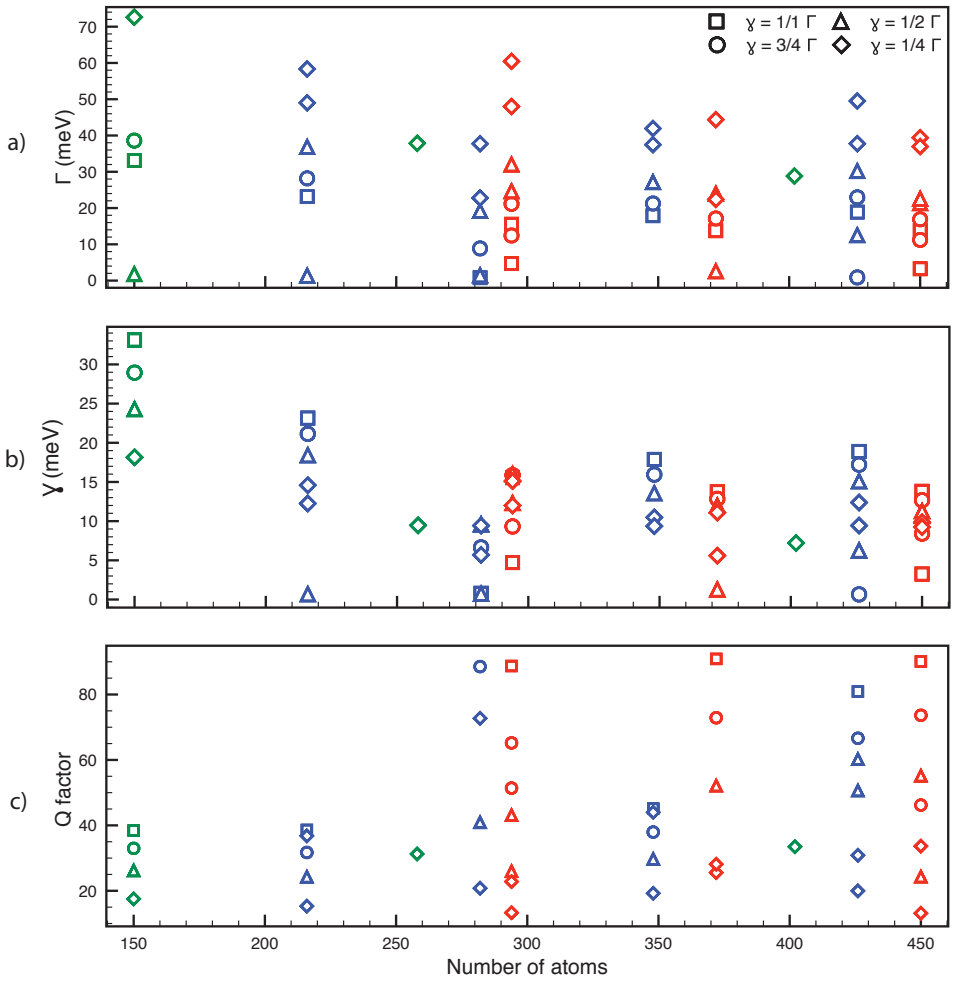

Figure 5. Calculations for the total inelastic damping rate 5(a), the phonon inelastic damping rate 5(b) and the Q-factor 5(c) for two different resonances. The *red*, *green* or *blue* color of the marker is linked to the family of resonances the disk belongs to. The symbol of the marker is related, according to the legend, to the γ/Γ ratio.

done in section 2: however, the physical insights and the main expressions have been summarized in it.

From equation (12) we could predict some results for the inelastic phonon damping rate γ. We have shown that, when the number of atoms of the structure increases, the phonon damping rate decreases, independently of the ratio between the phonons and the total damping rate γ/Γ, suggesting an small contribution from phonons to the plasmon damping for really large carbon planar structures. However, the current implementation of the equations above makes very difficult to simulate huge structures, because of computational limitations.

Acknowledgements

I would like to thank first Javier García de Abajo, my thesis advisor, for his guidance and patience throughout all this year. Also my sincere thanks to my colleagues from the Nanophotonics Theory group at ICFO. Finally, thanks to Josep Canals and Néstor Costa for the critical reading of this text.

References

[1] Zia, R., Selker, M. D., Catrysse, P. B. Brongersma, M. L. Geometries and materials for subwavelength surface plasmon modes. J. Opt. Soc. Am. A, JOSAA 21, 2442–2446 (2004).

[2] Prodan, E. Nordlander, P. Structural Tunability of the Plasmon Resonances in Metallic Nanoshells. Nano Lett. 3, 543–547 (2003).

[3] Stewart, M. E. et al. Nanostructured Plasmonic Sensors. Chem. Rev. 108, 494–521 (2008).

[4] Liu, Z., Steele, J. M., Srituravanich, W., Pikus, Y. Sun, C. Focusing surface plasmons with a plasmonic lens. Nano ... (2005). doi:10.1021/nl051013j

[5] Novotny, L. Van Hulst, N. Antennas for light. Nature Photonics (2011).

[6] Maier, S. A. Plasmonics: Fundamentals and Applications: Fundamentals and Applications. (Springer, 2007).

[7] Baffou, G., Quidant, R. Girard, C. Heat generation in plasmonic nanostructures: Influence of morphology. Appl. Phys. Lett. 94, 153109 (2009).

[8] García de Abajo, F. J. Graphene Plasmonics: Challenges and Opportunities. ACS Photonics 1, 135–152 (2014).

[9] Grigorenko, A. N., Polini, M. Novoselov, K. S. Graphene plasmonics. Nature Photonics (2012).

[10] Koppens, F. H. L., Chang, D. E. de Abajo, F. G. Graphene Plasmonics: A Platform for Strong Light–Matter Interactions. Nano Lett. 11, 3370–3377 (2011).

[11] Jablan, M., Buljan, H. Soljačić, M. Plasmonics in graphene at infrared frequencies. Phys. Rev. B 80, 245435 (2009).

[12] Bostwick, A., Ohta, T., Seyller, T., Horn, K. Rotenberg, E. Quasiparticle dynamics in graphene. Nat Phys 3, 36–40 (2006).

[13] Nakada, K., Fujita, M., Dresselhaus, G. Dresselhaus, M. S. Edge state in graphene ribbons: Nanometer size effect and edge shape dependence. Phys. Rev. B (1996).

[14] Mermin, N. D. Lindhard Dielectric Function in the Relaxation-Time Approximation. Phys. Rev. B B1, 2362–2363 (1970).

[15] Manjavacas, A., Marchesin, F. Thongrattanasiri, S. Tunable Molecular Plasmons in Polycyclic Aromatic Hydrocarbons - ACS Nano (ACS Publications). (2013).

[16] Wallace, P. R. The band theory of graphite. Physical Review (1947).

[17] Levine, I. N. Quantum chemistry. (Prentice Hall, 2009).

[18] Ashcroft, N. W. Mermin, N. D. Solid State Physics (Holt, Rinehart and Winston, New York, 1976).

[19] Sakurai, J. J. Tuan, S. F. Modern quantum mechanics. (Addison-Wesley, 1994).